

Dust Particle Removal by Electrostatic and Dielectrophoretic Forces with Applications to NASA Exploration Missions

C.I. Calle¹, J.L. McFall², C.R. Buhler², S.J. Snyder², E.E. Arens¹,
A. Chen³, M.L. Ritz², J.S. Clements⁴, C.R. Fortier¹, and S. Trigwell²

¹ NASA Electrostatics and Surface Physics Laboratory

Kennedy Space Center, FL 32899

Phone: (1) 867-3274

email: carlos.i.calle@nasa.gov

² ASRC Aerospace, Kennedy Space Center

³ Department of Physics, Oklahoma Baptist University

⁴ Department of Physics and Astronomy, Appalachian State University

Abstract— The dusty lunar environment can hinder NASA's exploration missions because of its ability to cling to most surfaces. The lunar dust is expected to be electrostatically charged due to solar UV irradiation and its exposure to the solar wind and to cosmic rays. As a result, NASA has an active dust mitigation program that is currently studying possible dust mitigation technologies. The Electrostatics and Surface Physics Laboratory at the Kennedy Space Center, in collaboration with several universities, has been working to develop an active dust mitigation technology for the last few years. In this paper, we report on our efforts to develop the Dust Shield, a dust removal technology that uses electrostatic and dielectrophoretic forces to remove dust already deposited on surfaces and to prevent the accumulation of dust particles approaching those surfaces. We also include results of computer simulations of charged particles interacting with these systems.

I. INTRODUCTION

The entire lunar surface is covered with a layer of dust with sizes in the micrometer and submicrometer range. This layer of dust is expected to be electrostatically charged for three main reasons. First, the moon has practically no atmosphere (it has a tenuous atmosphere with an atmospheric pressure in the 10^{-13} kPa range) and no magnetic field so that the high energy electrons and protons in the solar wind reach the surface completely unimpeded. Second, due to the relatively high surface and volume resistance of the lunar regolith and the complete lack of liquid water in the regolith, the charge decay of the lunar dust should approach infinity. Third, due to the lack of an atmosphere, the full

spectrum of the sun's electromagnetic radiation reaches the surface, charging the dust and also affecting its current charge state.

Charged and uncharged dust on the surface of the moon will present several challenges to manned and unmanned exploration missions currently being planned. Dust will adversely affect the operation of most mechanical systems required by these missions. Charged dust will be particularly difficult to remove from astronauts suits, gloves, and visors. Charged dust will also stubbornly adhere to solar panels and thermal radiators, thus decreasing their efficiencies.

We are developing an active dust mitigation technology that is proving very effective in the removal of dust particles from surfaces and in the prevention of the accumulation of those particles on such surfaces. The technology makes use of electrostatic and dielectrophoretic forces to move charged dust particles off surfaces and to prevent dust particles from depositing on those surfaces.

II. BACKGROUND AND THEORY

The dust removal technology described in this paper is based on the electric curtain concept developed by F.B. Tatom and collaborators at NASA in 1967 [1] and further developed by Masuda at the University of Tokyo in the 1970s [2-6]. This technique has been shown to lift and transport charged and uncharged particles using electrostatic and dielectrophoretic forces [7,8]. The technology has never been applied for space applications on the moon.

The Dust Shield consists of a series of parallel electrodes connected to an AC source that generate a traveling wave acting as a contactless conveyor (Fig. 1). Particles are repelled by the electrodes used to produce the field and travel along or against the direction of the wave, depending on their polarity. The curtain electrodes can be excited by a single-phase or a multi-phase AC voltage. In the single-phase electric curtain, parallel cylindrical electrodes connected to an AC voltage source generate an electric field whose direction oscillates back and forth as the polarity of the electrodes changes. In this case, a standing wave is produced which would generate a force on any charged particle in the region of the field.

Since the mesh of electrodes is usually covered with a thin insulating layer to increase the breakdown voltage, uncharged particles falling on the surface before the field is turned on may become charged by repeated contact with the insulating layer, if they bounce, or due to the electrophoretic force, and will be affected by the field once it is turned on. A multi-phase electric curtain produces a traveling wave, since the potential at each electrode changes in steps due to the phase shift. A charged particle in this region will move with or against this wave, depending on its polarity.

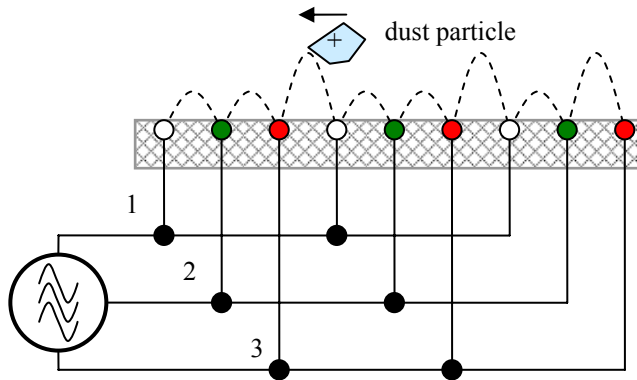


Fig. 1: Three-phase electric curtain.

The net force of repulsion on the particles, which levitates them above the surface, can be expressed as the contribution from the electrodynamic force, the viscous force, and the gravitational force:

$$M \frac{d^2 r}{dt^2} = qE \cos \omega t - 6\pi\eta \frac{dr}{dt} - mg$$

where m is the particle mass, r is the particle's position, η is the viscosity of the fluid in which the particles move, q is the particle charge, and g is the acceleration due to gravity

Due to the complicated nature of the particle-field interaction, where the motion of the particles is nonlinear and coupled, this equation of motion cannot be solved analytically. Masuda [9] proposed a solution to a linear approximation to the equation of motion assuming small oscillations for the particles. In addition, with a numerical solution to the equation of motion, he was able to obtain simulations of the particle motion which matched actual measurements of particle trajectories fairly well.

Although the forces responsible for the levitation of the particles are highly dependent on their charge, uncharged particles can ultimately be removed from the curtain as well. It has been well documented that polarizable particles can be levitated using these techniques [10]. Since many larger neutral particles contain nearly equal amounts of positive and negative charges on their surface, these particles possess an extrinsic electric dipole moment. If this dipole moment is exposed to a spatially non-uniform electric field, the particles will experience a force. Likewise, particles with intrinsic electric dipole moments or containing polar materials like water will also experience a force. The movement of particles with internal electric dipole moments in a non-uniform electric field is called the *dielectrophoretic force* [10]. All that is required for levitation is that the particles have a different dielectric constant than that of the surrounding medium. The time-averaged force of an electric dipole in a spatially (and time) dependent electric field is given by

$$\langle \vec{F} \rangle = \frac{1}{2} \text{Re}[(\vec{p} \cdot \vec{\nabla}) \cdot \vec{E}^*]$$

where \vec{E}^* is the complex conjugate of the electric field and \vec{p} is the induced electric dipole moment. For spherical particles the dipole moment becomes

$$\vec{p} = 4\pi\epsilon_m r^3 f_{\text{CM}} \vec{E}$$

where ϵ_m is the permittivity of the medium and f_{CM} is the Clausius-Mossotti factor given by:

$$f_{\text{CM}} = \frac{\epsilon_p^* - \epsilon_m^*}{\epsilon_p^* + 2\epsilon_m^*}$$

Here ϵ_p^* and ϵ_m^* are the complex permittivities of the particle and the medium, respectively. Combining the above equations yields the following result for the time-averaged dielectrophoretic force experienced by polarizable spherical particles:

$$\langle \vec{F} \rangle = \pi\epsilon_m r^3 \left[\text{Re}(f_{\text{CM}}) \nabla E^2 + 2 \text{Im}(f_{\text{CM}}) \nabla \times (\vec{E}_I \times \vec{E}_R) \right]$$

\vec{E}_I and \vec{E}_R are the negative gradients of the potentials ϕ_I and ϕ_R , while $\text{Re}(f_{\text{CM}})$ and $\text{Im}(f_{\text{CM}})$ are the real and imaginary parts of the Clausius-Mossotti factor, respectively [6]. This force not only applies to polarizable particles, but also to bipolar particles (those containing equal amounts of positive and negative charge) and this component should be added to the force equation. If the permittivities of the particles are less than that of the medium, the particles will move toward the point in which the field gradient is the smallest, i.e. away from the curtain. However, in a majority of cases, the particles have a higher dielectric constant than the surrounding medium and will be attracted to the curtain's electrodes. In this case, a neutral particle traveling along the insulated screen would triboelectrically acquire a charge and would then be lifted from the screen by the stronger qE force. Solving the equation of motion containing just the dielectrophoretic force alone is extremely difficult analytically and requires computational methods.

The dielectrophoretic force is commonly used for transportation of particles in a liquid medium [8], fluids through microchannels [5], blood cells [11] and other biological matter [12].

II. EXPERIMENTS

We have developed Dust Shield prototypes that can remove dust from surfaces and prevent dust accumulation [13-29]. Several types of Dust Shields were designed and built. Rigid, opaque shields in a dielectric substrate with metallic electrodes in parallel or spiral configurations; rigid, transparent shields on a dielectric substrate with transparent elec-

trodes in a parallel or spiral configuration; rigid, transparent shields in a dielectric coating on a metallic substrate with metallic electrodes in a parallel or spiral configuration; flexible, opaque shields on a dielectric substrate with flexible electrodes; and flexible, transparent shields on a dielectric substrate with flexible, transparent electrodes (Fig. 2).

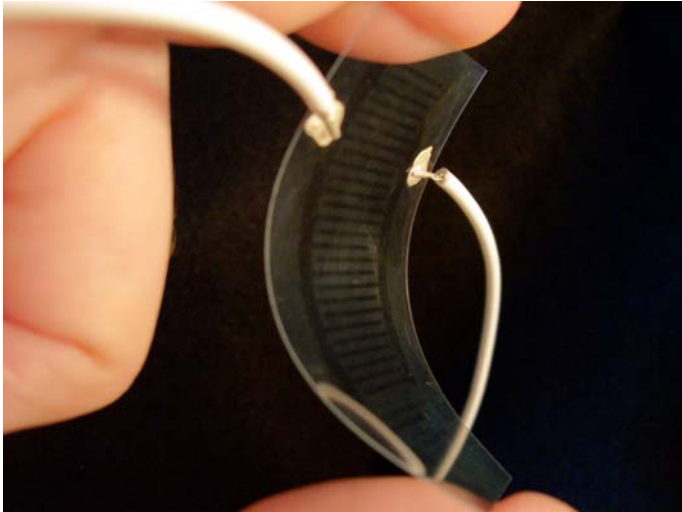


Fig.2. Transparent Dust Shield with transparent indium tin oxide (ITO) parallel electrodes.

A. Low Humidity Experiments at Ambient Conditions

The transparent shields used in our experiments use a three-phase spiral ITO electrode design, as shown in Fig. 3. Lunar simulant JSC-1A with particles of several size fractions ranging from under $10\ \mu\text{m}$ and 10 to $50\ \mu\text{m}$ was spread over the entire area covered by the electrode pattern. With this spiral pattern, the dust is moved radially outward and is deposited beyond the perimeter of the electrode pattern. Fig. 3 illustrated the dust shield before and after energizing. These dust shields were run in a glove box at 0% relative humidity to simulate the absence of water in the 10^{-13} kPa lunar atmosphere.



Figure 3. Transparent screen with a transparent ITO three-phase spiral pattern. (Left) The electrode area is covered with JSC-1A lunar simulant. (Right) The electrode area after energizing.

To obtain a proof of concept for the development of a prototype dust shield integrated on a metal surface, transparent shields like the one on Fig. 3 were placed in contact with a metal plate, as shown in Fig. 4. The concern was that the presence of the nearby metal plate would distort the electric fields generated by the electrodes and inactivate the shields. The shields were run with the same wave pattern and amplitude as the earlier shields shown in Fig. 3.

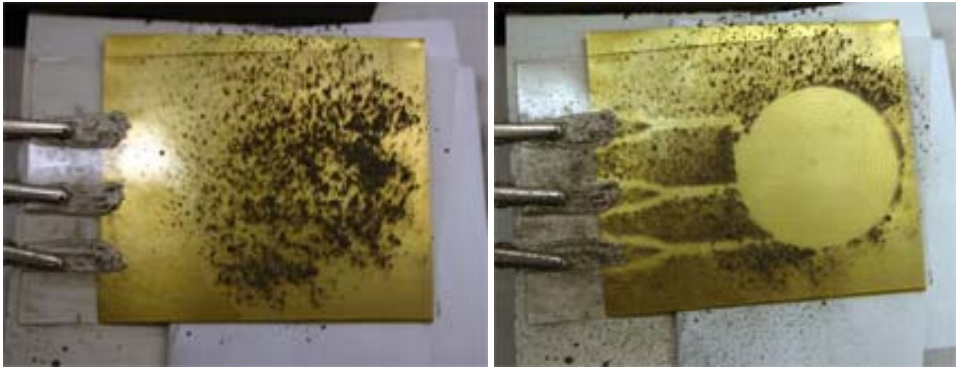


Fig. 4: Before and after photographs of a Dust Shield prototype on a metal plate to provide proof of concept for a sample handling system.

B. Experiments at High Vacuum

1) Solar Panels

Experiments with JSC-1A simulant were performed in a vacuum chamber at 10^{-6} kPa. The lunar simulant was kept in a vacuum for several days. Aerosolized simulant dust ($<20 \mu\text{m}$) was deposited on the shields under very low relative humidity conditions (Fig. 5). The shields were rapidly transferred to the chamber for testing. Although the simulant-covered shield was briefly exposed to ambient air at 50% relative humidity, we believe that the small amount of water absorbed was quickly removed when the chamber was promptly evacuated. All Dust Shields were three-phase and in the form of a spiral pattern to allow electrical contact to be made on one side of the surface.

Four Dust Shields were placed inside a stainless-steel high vacuum chamber in order to perform tests under simulated lunar vacuum conditions. The chamber pressure is monitored using two MKS Series PR 4000 vacuum gauges for pressures above 6 kPa and a Varian Ion Gauge for high vacuum ranges. The high vacuum was supplied using a Varian Model 300HT Turbo molecular pump, and the roughing vacuum is accomplished using a Varian 600 series scroll pump. Together the system is capable of reaching 10^{-7} kPa with tests typically performed at $5.0 \pm 2.0 \times 10^{-6}$ kPa.

Approximately 20 mg of dust is delivered to each Dust Shield by rapidly shaking a feeder cup 3.8 cm in diameter with a metal screen mesh at the bottom of the cup. The mesh sizes are chosen for their ability to contain dust without dropping particles until shaken. Typically, each grain size requires its own metal mesh. Shaking of the feeder cup occurs by engaging a vibrating motor fastened to the cup. Dust is deposited to the surface

of each shield individually while under vacuum conditions using two Micos translation stages (X and Y direction) controlled via LabView (National Instruments, Inc.). The translation stages position the shaker feeder over the shield, deposit dust, and move to the next shield. Once dust is deposited on all four shields, the stages are sent to the “home” position to allow visual inspection and videography of clearing efficiencies.

The demonstration of clearing efficiencies was performed by using simple 5 cm × 5 cm solar panels which supply between 3-4 volts initially. This voltage drop, though slight for laboratory testing of proof of concept, may be significant in a space-based photovoltaic system and needs further investigation to better match the optical characteristics of the shield layer to the solar panel. Aluminum foil cutouts were used to match the spiral pattern of the shields for efficiency measurements. A picture of the shields and feeder inside the vacuum chamber prior to dust deposition and pump down is shown in Fig. 5. The white background is a PTFE sheet used to electrically isolate the high voltage from the grounded chamber. The size fraction of the JSC-1A dust used for testing was 50-75 μm and did not require bake-out.

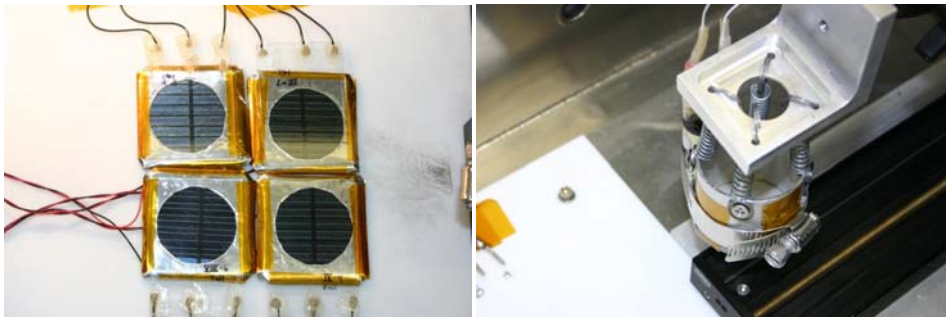


Fig. 5. (Left) Solar panel-backed transparent Dust Shields used for testing at high vacuum conditions. (Right) Feeder cup used to deliver dust to the Dust Shields in the vacuum chamber.

Fig. 6 shows the solar panel response throughout the experiments such as the initial voltage readings of the four panels, the voltage readings as a result of dust deposition, and subsequent removal. The time offset in voltage level drop for each panel coincides with the time it took for the feeder cup to deliver dust to each shield individually.

The deposition of JSC-1A dust corresponds to a significant drop in output voltage for each solar panel. The voltage output typically drops to or below 20% of its initial voltage and remains constant in time. Once the electrodynamic shields are turned on, the efficiencies raise quickly to above 90% within the first two minutes and improve gradually in time. Measurements of the output efficiency taken upon dust loading, two minutes after shield activation and half-an-hour after activation are highlighted in Table 1.

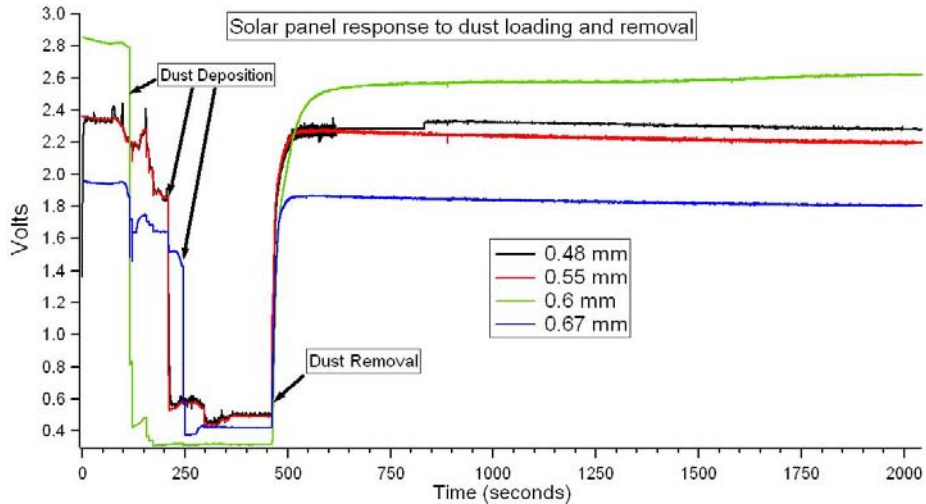


Fig.6. Solar panel response to 50-75 μm JSC-1A dust deposition and removal under high vacuum conditions. Removal was accomplished using Dust Shields of four different electrode spacings: 0.48 mm, 0.55 mm, 0.6 mm, and 0.67 mm.

The first column in Table 1 shows the reduced efficiencies as a function of dust loading for each of the four shields. Dust loading is typically quite dramatic since the solar panel cannot be seen visually beneath the dust layer. After the shields are activated, the voltage recovers to above typically 90% and continues to increase gradually with time. The error in the data is on the order of 1-2 %

TABLE 1: SOLAR PANEL EFFICIENCIES

| Solar Panel | Efficiency with Dust Deposition | Efficiency after 2 minutes of Shield Activation | Efficiency after $\frac{1}{2}$ hour of Shield Activation |
|-------------|---------------------------------|---|--|
| 0.48 mm | 20.3 % | 99.4 % | 98.3 % |
| 0.55 mm | 19.3 % | 98.7 % | 98.6 % |
| 0.6 mm | 11.0 % | 91.6 % | 99.1 % |
| 0.67 mm | 22.5 % | 98.4 % | 98.1 % |

From the data above, it is apparent that the Dust Shield can be made transparent and operate successfully under high vacuum conditions even under extreme dust loading conditions. Efficiencies above 98% should be accomplished easily upon final design. The application of the Dust Shields did not seem to have any adverse effects on the solar panels themselves. Further analysis will have to be performed to determine any electromagnetic interference (EMI) or electromagnetic compatibility (EMC) issues that may arise when the shield technology is incorporated into a full photovoltaic system. The radiated fields from the dust shield are low power which should limit any adverse effects.

2) Rigid, Transparent Dust Shields

Hundreds of tests were performed on transparent Dust Shields under high vacuum in order to understand its capabilities and limitations (Fig. 7). Cleaning efficiencies were determined qualitatively using visual estimation methods for each test. Dust removal ceases to occur a short time after activation. Once macroscopic dust movement is no longer visible, the system is turned off and efficiencies are estimated. Dust deposited onto or over the edge of the spiral pattern is not included in determining efficiencies. Although this method for determining efficiencies is highly imprecise, it can be argued that it is *accurate* within $\pm 5\%$. Its advantages are that it serves well for comparing several runs and greatly reduces testing time for hundreds of tests. More advanced techniques can be used later to enhance accuracy after trends are discovered. For the purposes of solar panels, which are very forgiving in terms of less stringent cleaning requirements (i.e. the solar panels on the Mars Rovers), the method serves well here, while other techniques would be necessary for measuring removal efficiencies such as the need for accounting for individual micron-sized particles that would hinder optical systems such as telescopes and imagers.

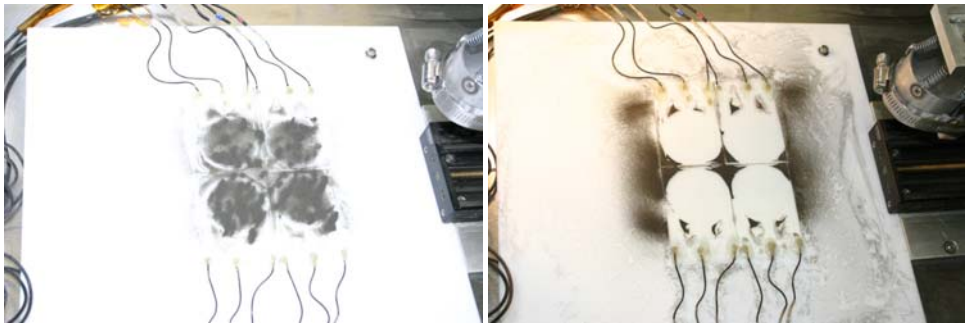


Fig. 7. Transparent Dust Shields with JSC-1A lunar simulant (50-75 micron) deposited under high vacuum conditions on transparent Dust Shields. (c) Dust removal after activation of the Dust Shields with efficiencies greater than 99%.

These tests serve to deliver a wealth of information in a short period of time. Parameters such as dust size, moisture content, high and low dust loading, voltage levels, frequencies, are all parameters that can and need to be evaluated quickly to optimize the technology. For example, the answer to simple questions such as the effect of moisture on the surface of the particles can be found quickly.

Using this method, we have classified the best removal efficiencies for transparent shields under high vacuum conditions using the entire range of sizes of JSC-1A simulant as a function of electrode spacing. The JSC-1A lunar simulant was sieved and used for testing purposes. Size fractions below $50\ \mu\text{m}$ required vacuum bake-out prior to testing to remove capillary forces between particles. Samples were typically heated above 180°C for several days at pressures less than $0.1\ \text{kPa}$. Larger size fractions did not require bake-out and did not conglomerate. Simulant was sieved using a Topac RP09 Digital Sieve

Shaker in several size fractions including particle diameters $a < 10 \mu\text{m}$, $a < 50 \mu\text{m}$, 50-100 μm , 100-180 μm , 180-200 μm , 200-280 μm , 280-300 μm , 300-400 μm , 400-450 μm and $a > 450 \mu\text{m}$. The results for ITO shields of trace widths between 0.3-0.4 mm and spacings of 0.48, 0.55, 0.6 and 0.67 mm are given in graphical in Fig. 8.

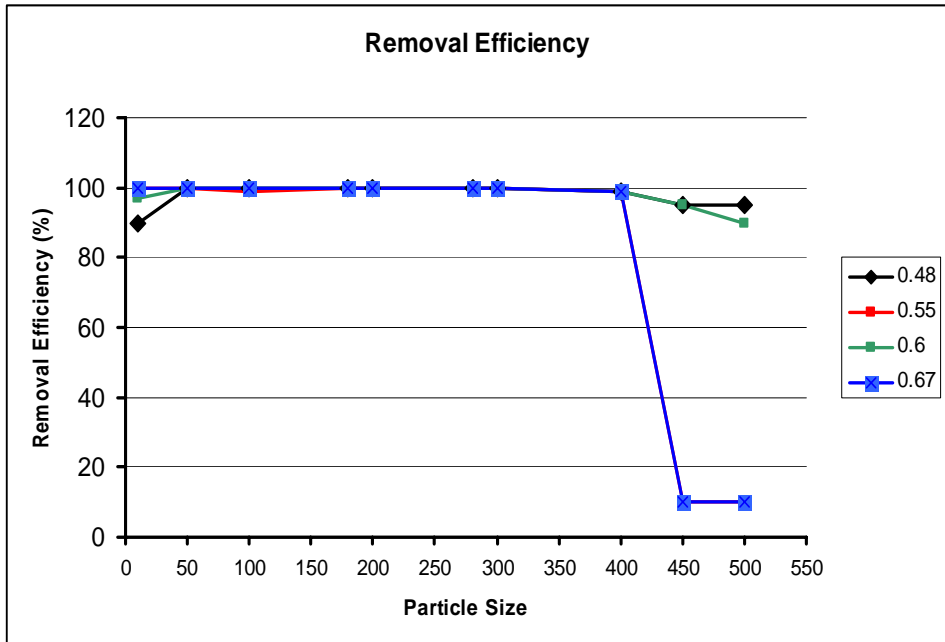


Fig. 8. (Left) Removal efficiency of JSC-1A as a function of particle size at lunar conditions.

3) Flexible Dust Shields on Fabric

Prototypes of flexible electrodes in a fabric substrate have been developed and tested with JSC-1A lunar simulant both at ambient and at high vacuum conditions. The initial tests were successful in removing dust from the fabric (Fig. 9). Further development of the prototypes to optimize electrode deposition and configuration is ongoing and will be reported in a future paper.



Fig. 9. Before and after photographs of a dust shield on fabric with JSC-1A lunar simulant.

III. NUMERICAL MODELING

The purpose of the modeling work presented here is to research and to better understand the physics governing the electrodynamic shield, as well as to advance and to support the experimental dust shield research. The numerical modeling employed a finite-element method to calculate the potentials and electric fields over the entire plane with 12 electrodes embedded in a layer of an insulating dielectric medium. With these values, dust particles trajectories were calculated. The time integration was done by using the Huen-Verlet scheme over a fixed time domain.

Fig. 10 shows electric field and equipotential lines for a 900-V three-phase square wave signal. Fig. 11 shows trajectory calculations for twelve charged dust particles moving on eight three-phase sine and square wave signals at an amplitude of 900 V.

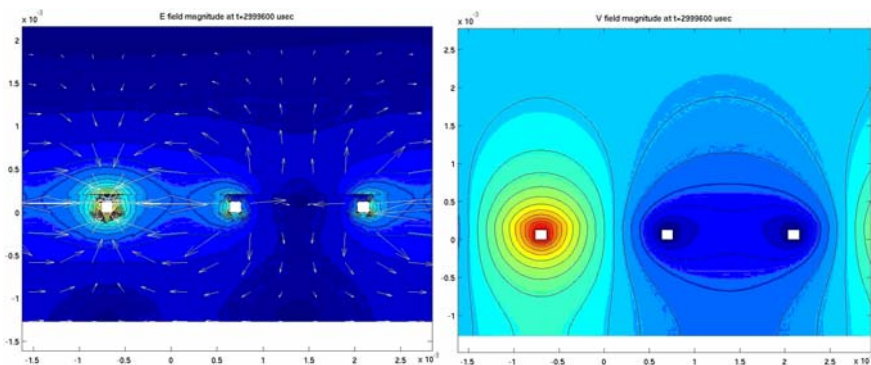


Figure 10: (Left) E-field configuration for a three-phase square signal, E-field plot. (Right) Electrostatic potential configuration.

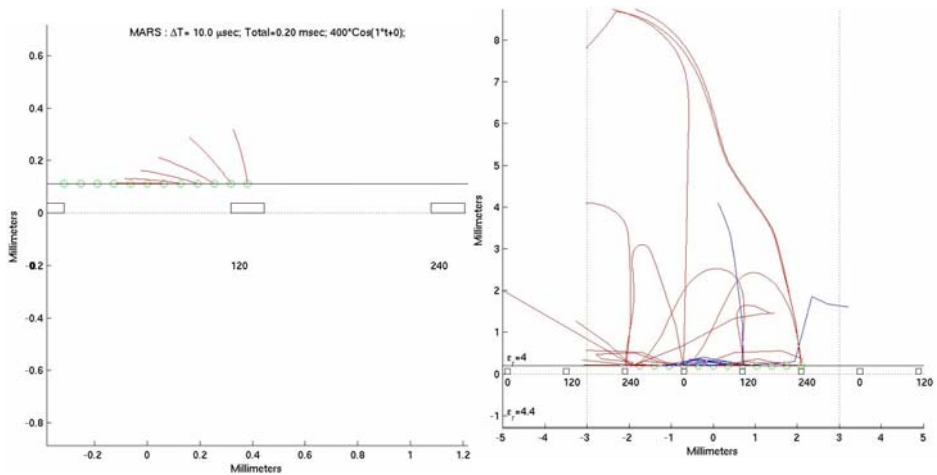


Fig. 11. (Left) Trajectory calculation of charged dust particles over 8 three-phase sine signals at 900 V. (Right) Trajectory calculation for 12 charged dust particles (the green circles indicate dust particle location) over 8 three-phase square signals at 900 V.

IV. CONCLUSION

Lunar exploration missions may be hindered by the presence of highly charged lunar dust that will adhere electrostatically to the surfaces of equipment, viewports, optical systems, instrumentation, and spacesuits. In this paper, we have reported on an active dust removal and prevention system that we have been developing over several years. The dust shield systems in development protect rigid opaque dielectric surfaces, rigid transparent surfaces such as solar panels, windows, and optical filters, metallic surfaces, and fabrics for spacesuits. Extensive testing at near zero relative humidity and at high vacuum (at least 10^{-6} kPa) shows that high efficiencies can be achieved with these systems.

Further development of these systems continues. We are currently concentrating on the optimization of the different techniques that we have developed. We will report on the results of such optimization in future papers.

ACKNOWLEDGEMENTS

This work has been funded by NASA's Exploration Technology Development Program and by the Kennedy Space Center Director Discretionary Fund. The authors wish to also acknowledge the support of Nancy Zeitlin and Karen Thompson at KSC.

REFERENCES

- [1] Tatom, F.B., V. Srepol, R.D. Johnson, N.A. Contaxes, J.G. Adams, H. Seaman, and B.L. Cline, "Lunar Dust Degradation Effects and Removal/Prevention Concepts", *NASA Technical Report No. TR-792-7-207A*, p. 3-1 (1967).

- [2] Masuda, S., *Advances in Static Electricity*, **1**, Auxilia, S.A., Brussels, 398 (1970)
- [3] Masuda, S. Fujibayashi, K., Ishida, K., and Inaba, H., *Electronic Engineering in Japan*, **92**, 9 (1972).
- [4] Masuda, S., and Matsumoto, Y., *Proc. of the 2nd International on Static Electrification*, Frankfurt (1973)
- [5] Masuda, S., Washizu, M., Kawabata, I., "Movement of Blood Cells in Liquid by Nonuniform Traveling Field", *IEEE Transactions on Industrial Applications*, **24**, No. 2, pp. 217-222 (1988)
- [6] Aoyoma, M., and Masuda, S., "Characteristics of electric dust collector based on electric curtain", Proceedings of the General Conference of the Institute of Electronic Engineers in Japan, No. 821 (1971)
- [7] Malnar, B., Balachandran, W., and Cecelja, F., "3D simulation of traveling wave dielectrophoretic force on particles", *Proceedings of the ESA-IEEE Joint Meeting on Electrostatics 2003*, Laplacian Press, Morgan Hill, CA, pp. 361-373 (2003)
- [8] Malyar, B., Kulon, J., and Balachandran, W., "Organization of particle sub-populations using dielectrophoretic force", *Proceedings of the ESA-IEEE Joint Meeting on Electrostatics 2003*, Laplacian Press, Morgan Hill, CA, pp. 313-322 (2003)
- [9] Masuda, S., "Electric Curtain for Confinement. and. Transport of Charged Aerosol Particles", *Proc. of Albany Conference on Electrostatics*, (1971)
- [10] Jones, T.B., *Electromechanics of Particles*, Cambridge University Press, Cambridge (1995)
- [11] Moesner, F.M. and Higushi, T., "Devices for particle handling by an AC electric field," *Proceedings of IEEE Micro Electro Mechanical Systems*, **66** pp. 66-71 (1995)
- [12] Zhou, G. Imamura, M., Suehiro, J., and Hara, M., "Enrichment and Recovery of Biological Cells Using a Dielectrophoretic Filter", *Proceedings of the ESA-IEEE Joint Meeting on Electrostatics 2003*, Laplacian Press, Morgan Hill, CA, pp. 337-348 (2003)
- [13] Sims, R.A., Biris, A.S., Wilson, J.D., Yurteri, C.U., Mazumder, M.K., Calle, C.I., and Buhler, C.R., "Development of a Transparent Dust Shield for Solar Panels" *Proc. of the ESA-IEEE Joint Meeting on Electrostatics 2003*, Laplacian Press, Morgan Hill, CA, 814 (2003)
- [14] Calle, C.I., C.R. Buhler, J.G. Mantovani, S. Clements, A. Chen, M.K. Mazumder, A.S. Biris and A.W. Nowicki, "Electrodynamic Shield to Remove Dust from Solar Panels on Mars," Proceedings of the 41st Space Congress (2004)
- [15] Calle, C.I., C.R. Buhler, J.G. Mantovani, S. Clements, A. Chen, M.K. Mazumder, A.S. Biris, and A.W. Nowicki, "Electrodynamic Dust Shield for Solar Panels on Mars, Lunar and Planetary Science XXXV, 2014 (2004)
- [16] Biris, A.S, D. Saini, P.K. Srirama, M.K. Mazumder, R.A. Sims, C.I. Calle, and C.R. Buhler, "Electrodynamic removal of contaminant particles and its applications," *Conference Record of the IEEE Industry Applications Conference*, Vol. 2, 1283-1286 (2004)
- [17] Biris, A.S., R.A. Sims, J.D. Wilson, M.K. Mazumder, C.I. Calle, C.R. Buhler, "Transparent Self-Cleaning Shield for Solar Panels," IEEE Industrial Applications Transactions, (2004)
- [18] Calle, C.I., "Dust Shield Technology for Lunar and Mars Exploration Activities," *Space Operations Communicator*" (2004)
- [19] Calle, C.I., C.R. Buhler, J.G. Mantovani, S. Clements, A. Chen, M.K. Mazumder, A.S. Biris, A.W. Nowicki, "Electrodynamic dust shield for solar panels on Mars," Workshop on Granular Materials in Lunar and Martian Exploration, Kennedy Space, Center, FL (2005)
- [20] Calle, C.I., A. Chen, J. Meyer, B. Linell, C.R. Buhler, S. Clements, and M.K. Mazumder, "Numerical modeling of an electrostatic dust shield for the Martian and lunar environments," *Earth and Space 2006*, Houston (2006)
- [21] Chen, A., J. Meyer, C.I. Calle, B. Linell, C.R., Buhler, S. Clements, and M.K. Mazumder, "Numerical and analytical model of an electrodynamic screen for solar panels on Mars," Lunar and Planetary Science XXXVII, 1873 (2006)
- [22] Immer, C., C.I. Calle, M.M. Michalenko, J. Starnes, and M. Ritz, "Electrostatic screen for transport of Martian and lunar regolith," *Proceedings of the Fifth World Congress on Particle Technology*, Orlando, FL (2006)
- [23] Calle, C.I., C. Immer, J.S. Clements, C. Buhler, A. Chen, J. Mantovani, P. Lundeen, and M. Michalenko, "Electrodynamic dust shield for surface exploration activities on the moon and Mars," *Proceedings of the International Astronautical Congress*, Valencia, Spain (2006)
- [24] Mazumder, M., M. Zahn, R. Sharma, J. Zhang, C.I. Calle, C. Immer, and N. Mardesich, "Development of self-cleaning dust shields using low-power electrodynamic fields for solar panels on Mars," *Proceedings of the 2006 ESA/IEJ/IEEE-IAS/SFE Joint Conference on Electrostatics*, Laplacian Press, Morgan Hill, CA (2006)

- [25] Clark, P.E., C.I. Calle, S.A. Curtis, J.F. Keller, F. Minetto, and J.G. Mantovani, "Electrostatic dust control on planetary surfaces," *Proceedings of the Space Technologies and Utilization Forum*, Albuquerque (2007)
- [26] Calle, C.I., J.G. Mantovani, C.R. Buhler, A. Chen, J.S. Clements, S. Trigwell, E.E. Arens, J.M. McFall, and M.L. Ritz, "Dust Mitigation Technologies for Lunar Exploration," *Proceedings of the International Conference on Exploration and Utilization of the Moon*, Sorrento, Italy (2007)
- [27] Mantovani, J.G. and C.I. Calle, "Controllable transport of particulate materials for in situ characterization," *Proceedings of the 2007 IEEE Aerospace Conference*, Big Sky, Montana (2007)
- [28] Calle, C.I., M.K. Mazumder, C.D. Immer, C.R. Buhler, J.S. Clements, P. Lundeen, A. Chen, and J.G. Mantovani, "Controlled particle removal from surfaces by electrodynamic methods for terrestrial, lunar, and Martian environmental conditions," *Proceedings of Electrostatics 2007*, University of Oxford, UK, March 25-29, 2007
- [29] Calle, C.I., J.S. Clements, C.R. Buhler, J.G. Mantovani, A. Chen, E.E. Arens, J.M. McFall, and M.L. Ritz, "Mitigation of Lunar Dust in Mechanical Systems," *Proceedings of the Space Technologies and Applications International Forum*, Albuquerque (2008).